



ELSEVIER

October 1994

Optical Materials 3 (1994) 269–274



Luminescence quantum efficiency of F_2^- and F_3^- centers in LiF crystals

Marcos Duarte, Izilda M. Ranieri, Martha M.F. Vieira

Instituto de Pesquisas Energéticas e Nucleares, P.O. Box 11049, São Paulo, Brazil

Received 1 April 1994; revised manuscript received 1 June 1994

Abstract

F_2^- color center in LiF crystals is a unique specie of color centers concerning its photothermal stability, its broad absorption band, centered at $0.96 \mu\text{m}$, and its broad emission band peaking at $1.12 \mu\text{m}$, being a tunable laser operating in the range from $1.08 \mu\text{m}$ to $1.22 \mu\text{m}$. The luminescence quantum efficiency of the main transition in the laser optical cycle was determined, at room temperature, and its value is 0.5 ± 0.1 . This value was obtained using a method correlating the absorption, excitation and photoacoustic spectra. Besides, the luminescence quantum efficiency of the fundamental transition of the F_3^- color center was determined. Also was estimated the energy transfer efficiency due to the overlapping of the F_3^- center emission and the F_2^- center absorption bands. Possible nonradiative deexcitation mechanisms accounting for the small luminescence quantum efficiency of the F_2^- color centers in LiF are also discussed.

1. Introduction

Color center lasers represent a very important class of light sources, due to their tunability, covering a very broad spectral region, and their capability of short pulse generation. In particular, the laser active medium F_2^- color center in the LiF matrix presents very good photothermal stability, even at room temperature [1], allowing high intensity optical excitation without destruction of the centers involved in the laser transition. It can be used for obtaining Q -switching and mode-locking regimes of Nd lasers. The laser action in LiF: F_2^- was attained for the first time in 1978 in the pulsed mode and in 1981 in the CW mode. This laser is tunable from 1.08 to $1.25 \mu\text{m}$, and using a mode-locked neodymium-glass laser as the pump source, subpicoseconds pulses could be obtained [1]. All these results were obtained at room temperature. F_3^- centers are also present in LiF, in the neighborhood of the F_2^- centers; they present nonlinear ab-

sorption of light and are not a laser active medium due to their low thermal stability [2,3]. These two centers present a mechanism of energy transfer due to the overlapping of the F_3^- center emission and the F_2^- center absorption bands.

In this paper the determination is reported of the Luminescence Quantum Efficiency (LQE) for F_2^- and F_3^- centers in LiF crystals at room temperature. The LQE, defined as the ratio between the emitted to the absorbed photons number in a given excitation, is important for the laser development, concerning optical pumping efficiency determination, for example, as well as for the basic understanding of the optical system. The understanding of physical processes, like radiative and nonradiative decay, is still very poorly known for this specie. The LQE parameter determination is not a straightforward measurement, and the majority of the employed models introduces a large uncertainty in the obtained values. Among these models one can point out the calori-

metric ones, that are practical and comprehensive. The models based on the photoacoustic effect are, in general, more sensitive [4–7].

The basic principle of the photoacoustic effect is simple to understand [8]: when a material is excited by a modulated light beam, the nonradiative deexcitation component generates heat, giving rise to a pressure wave propagating from the excitation region throughout the material. This pressure wave follows the same modulation frequency as the illumination beam and can be detected by a microphone or a piezoelectric transducer.

2. Theory

The luminescence quantum efficiency (LQE) for an optical transition in a sample excited with monochromatic light (λ) is defined as the ratio

$$\eta(\lambda) = \sum_{\lambda_e} N_e(\lambda_e) / N_a(\lambda), \quad (1)$$

where N_e is the number of emitted photons with wavelength λ_e and N_a is the number of absorbed photons with the excitation wavelength λ .

The conversion efficiency of the absorbed luminous energy (E_a) into thermal energy (E_T) is defined as

$$F(\lambda) = \frac{E_T}{E_a} = \frac{E_a - E_c}{E_a} = \frac{hN_a(\lambda) c/\lambda - \sum_{\lambda_e} hN_e(\lambda_e) c/\lambda_e}{hN_a(\lambda) c/\lambda}, \quad (2)$$

$$F(\lambda) = 1 - (\lambda/\bar{\lambda}_e)\eta(\lambda), \quad (2a)$$

where h is Planck's constant, c is the velocity of light and $\bar{\lambda}_e$ is the wavelength of the maximum of the emission band; in other words, E_c is calculated as $E_c = (hc/\bar{\lambda}_e) \sum_{\lambda_e} N_e(\lambda_e)$.

The LQE can then be written as

$$\eta(\lambda) = (\bar{\lambda}_e/\lambda) [1 - F(\lambda)] \quad (3)$$

showing that the LQE can be calculated from $F(\lambda)$.

The intensity of a photoacoustic (PA) signal generated in a sample illuminated with chopped monochromatic light (λ) can be described as [5]

$$i_{PA}(\lambda) = Ai_0(\lambda) \{1 - \exp[-\beta(\lambda)l]\} F(\lambda), \quad (4)$$

where $i_0(\lambda)$ is the beam intensity incident on the sample, $\beta(\lambda)$ is the optical absorption coefficient of the sample, l is the sample thickness and A is a function dependent on the geometric parameters of the photoacoustic cell, on the thermal properties of the sample and the gas, and on the microphone sensitivity (more details in the experimental). For a fixed geometry, sample and transducer, A is a constant representing the cell sensitivity.

On the other side, the excitation signal intensity can be written as [5]

$$i_{EX}(\lambda) = Bi_0 \{1 - \exp[-\beta(\lambda)l]\} [1 - F(\lambda)], \quad (5)$$

where B is a function dependent on the experimental arrangement and on the optical properties of the sample, being also a multiplicative factor.

The signals obtained (i_{PA} and i_{EX}) were corrected concerning the whole system spectral response (lamp plus monochromator). This was done using a total absorber as sample in the PA cell to obtain the light intensity incident on the sample. Thus, there is no wavelength dependence on the constants A and B .

The addition of Eqs. (4) and (5) gives

$$\frac{I_{PA}(\lambda)}{A} + \frac{I_{EX}(\lambda)}{B} = 1 - \exp[-\beta(\lambda)l], \quad (6)$$

where $I_i(\lambda) = i_i(\lambda)/i_0(\lambda)$ are the normalized intensities.

The methodology employed in the LQE determination needs the three spectra, photoacoustic ($I_{PA}(\lambda)$), excitation ($I_{EX}(\lambda)$) and absorption ($\beta(\lambda)$) spectra. If the three spectra are known the absolute values for A and B can be evaluated by fitting Eq. (6) for several wavelengths. To avoid background problems one can do the following [5]:

$$\frac{I_{PA}(\lambda_1) - I_{PA}(\lambda_2)}{A} + \frac{I_{EX}(\lambda_1) - I_{EX}(\lambda_2)}{B} = \exp[-\beta(\lambda_1)l] - \exp[-\beta(\lambda_2)l], \quad (7)$$

where λ_1 and λ_2 are different wavelengths. To get a good statistics several different values for λ_1 and λ_2 were used to adjust A and B . In a simplified notation Eq. (7) can be rewritten as

$$\frac{\Delta I_{PA}}{A} + \frac{\Delta I_{EX}}{B} = \Delta\beta. \quad (7a)$$

Once the A and B values are known, the LQE can be obtained from

$$\eta(\lambda) = \frac{\bar{\lambda}_e}{\lambda} \frac{I_{\text{EX}}(\lambda)/B}{I_{\text{EX}}(\lambda)/B + I_{\text{PA}}(\lambda)/A}. \quad (8)$$

3. Experimental

The LiF crystals were grown by the Czochralski method. Four samples were studied. These samples were cut and polished in the following dimensions: $1 \times 1 \times 0.25 \text{ cm}^3$ (samples 1 and 4) and $1 \times 1 \times 2 \text{ cm}^3$ (samples 2 and 3). Samples 1 and 4 were grown at our crystal growth laboratory and samples 2 and 3 were grown at the General Physics Institute, Russia. Sample 1 was electron-irradiated and samples 2, 3 and 4 were γ -irradiated.

The optical absorption spectra were obtained using a Cary 17D spectrophotometer and the excitation spectra were obtained collecting the emitted light using a right angle optical path, in the same arrangement used for the photoacoustic experiment. Special care was taken to avoid autoabsorption of the F_2^- centers by making the excitation light incident on the border of the sample, since there is a small Stokes shift between the absorption and the emission spectra.

The PA measurements were done employing an experimental apparatus where the light from a tungsten filament halogen lamp was sent through a 0.25 m monochromator and then modulated by a chopper. The light beam was then focused onto the sample in the photoacoustic cell; the PA signal was amplified by a lock-in amplifier and then registered. The tungsten lamp was chosen due to its flat emission in the process, that was previously obtained using a photoacoustic cell containing a wavelength independent absorber (carbon black). Reproducible results were obtained normalizing the results of the measurements with respect to the spectral response of the apparatus. A spectral resolution of 20 nm was used to provide enough light intensity in the samples (the resolution does not affect the measurements due to the broad emission bands of the F_2^- and F_3^- centers). The PA cell was designed and built at our facilities (Fig. 1). It is an open photoacoustic cell made out of Plexiglas, in a configuration where the sample acts as window for the cell, with indirect detection of the PA

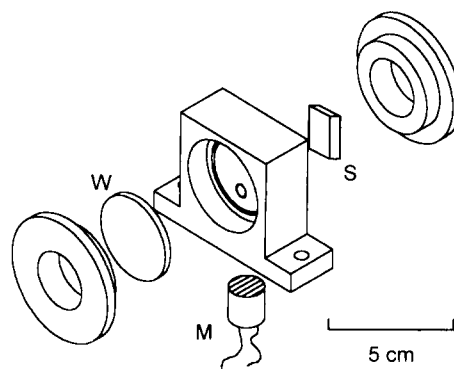


Fig. 1. Schematic drawing of the photoacoustic cell (S – sample; M – microphone; W – window).

signal. The volume of the cell is around 60 mm^3 . The detection element is a low cost electret microphone with $-65 \pm 4 \text{ dB}$ sensitivity (0 dB REF $1 \text{ V}/\mu\text{bar}$ at 1 kHz). When carbon black was used as absorbing material in the PA cell a 0.5 V/W sensitivity was observed in the system. The modulation frequency chosen was 40 Hz, due to the better signal to noise ratio and the time constant of the lock-in amplifier was set to 30 s.

4. Results

4.1. Luminescence quantum efficiency for $\text{LiF}:F_2^-$

All the obtained spectra were decomposed in gaussians in order to obtain the F_2^- band isolated from the bands due to other color centers located near the F_2^- center.

The optical absorption spectra obtained for the four samples studied are shown in Fig. 2. It can be seen that the absorption intensity for the F_2^- centers is of the same order as for the F_3^- centers. Up to now it was not possible to obtain high concentrations of isolated F_2^- centers and thus to avoid absorption of the species in the pump wavelength. Sample 4 presents the highest ratio between the absorption coefficients for the F_2^- and F_3^- centers and this sample is laser active in the pulsed regime [9].

The optical excitation spectra were obtained monitoring the band emission of F_2^- centers peaking at

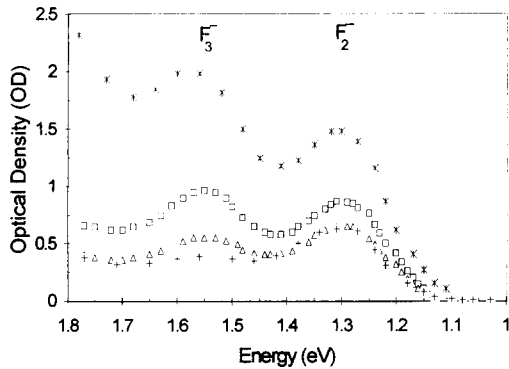


Fig. 2. Optical absorption spectra of the four LiF:F₂⁻ samples studied. Sample 1: X; Sample 2: □; Sample 3: △; Sample 4: +.

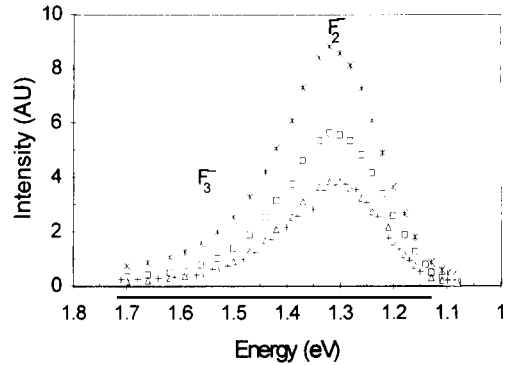


Fig. 4. Photoacoustic spectra of the four LiF:F₂⁻ samples studied. Sample 1: X; Sample 2: □; Sample 3: △; Sample 4: +.

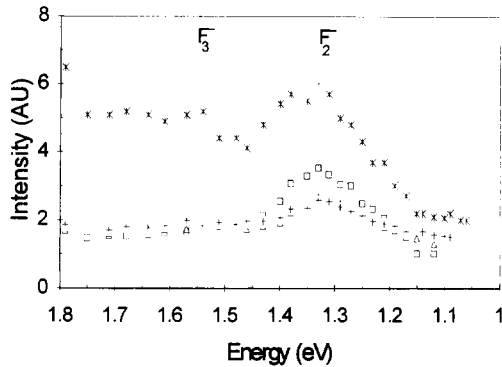


Fig. 3. Excitation spectra of the four LiF:F₂⁻ samples studied. Sample 1: X; Sample 2: □; Sample 3: △; Sample 4: +.

1.11 eV (1.12 μm), presented in Fig. 3. One can see the band due to the F₂⁻ centers peaking at 1.29 eV (0.96 μm) and at 1.55 eV (0.80 μm) the band due to the energy transfer from the F₃⁻ centers, that absorb at 1.55 eV and emit at 1.39 eV (0.89 μm), to the F₂⁻ centers.

The photoacoustic spectra obtained can be seen in Fig. 4. It is observed that the photoacoustic signal intensity for the F₂⁻ centers is much higher than for the F₃⁻ centers, although both centers present very similar optical absorption, foreseeing a different luminescent quantum efficiency for them.

Considering the three spectra (absorption, excitation and photoacoustic) and Eq. (7a) one can obtain $\Delta I_{EX}/\Delta\beta$ against $\Delta I_{PA}/\Delta\beta$ as shown in Fig. 5 for each sample studied. With the values for the constants *A* and *B* obtained from Fig. 5 and using Eq. (8) it was

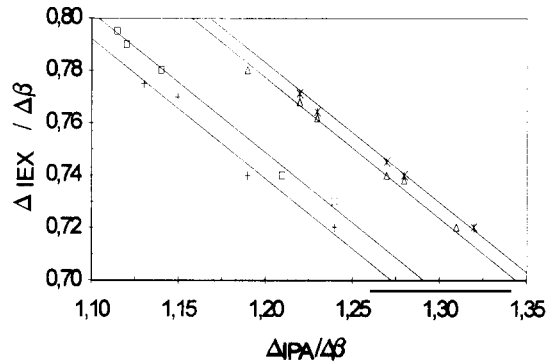


Fig. 5. Plot of $\Delta I_{EX}/\Delta\beta \times \Delta I_{PA}/\Delta\beta$ for the four LiF:F₂⁻ samples studied. Sample 1: X; Sample 2: □; Sample 3: △; Sample 4: +.

Table 1
Luminescence quantum efficiency (LQE) for LiF:F₂⁻ crystals

Sample	LQE(η)
#1	0.4 ± 0.1
#2	0.5 ± 0.1
#3	0.5 ± 0.1
#4	0.5 ± 0.1

possible to calculate the LQE values, presented in Table 1.

4.2. Luminescence quantum efficiency for LiF:F₂⁻

Using the luminescence quantum efficiency obtained for the F₂⁻ centers and the obtained spectra it

was possible to estimate the luminescence quantum efficiency for the F_3^- centers. Initially the energy transfer from the F_3^- to the F_2^- centers was disregarded.

The intensity of the normalized photoacoustic signals generated by the F_2^- and F_3^- centers can be written respectively as (see Eq. (4))

$$I_{PA,F_2^-}(\lambda) = A \{1 - \exp[-\beta_{F_2^-}(\lambda)l]\} F_{F_2^-}(\lambda), \quad (9)$$

$$I_{PA,F_3^-}(\lambda') = A \{1 - \exp[-\beta_{F_3^-}(\lambda')l]\} F_{F_3^-}(\lambda'). \quad (10)$$

From the ratio of Eq. (9) to Eq. (10) one obtains

$$F_{F_3^-}(\lambda') = \frac{I_{PA,F_3^-}(\lambda') \{1 - \exp[-\beta_{F_2^-}(\lambda)l]\}}{I_{PA,F_2^-}(\lambda) \{1 - \exp[-\beta_{F_3^-}(\lambda')l]\}} F_{F_2^-}(\lambda). \quad (11)$$

Having a value for $F_{F_3^-}(\lambda)$ one can get the luminescence quantum efficiency using Eq. (3) and the data from the absorption and the photoacoustic spectra. The obtained values are shown in Table 2.

If the energy transfer from the F_3^- to the F_2^- centers is considered, a different calculation has to be done. Considering that in the energy transfer mechanism there is absorption at the F_3^- center (1.55 eV), emission from the F_3^- center (1.39 eV), absorption at the F_2^- center (1.29 eV) and emission from the F_2^- center (1.11 eV), then the PA signal intensity generated by the F_3^- center will be added up by

$$I_{PA,F_3^- \rightarrow F_2^-}(\lambda) = A \{1 - \exp[-\beta_{F_3^-}(\lambda)l]\} \times [1 - F_{F_3^-}(\lambda)] \{1 - \exp[-\beta_{F_2^-}(\bar{\lambda})l]\} F_{F_2^-}(\bar{\lambda}), \quad (12)$$

where $I_{PA,F_3^- \rightarrow F_2^-}(\lambda)$ is the photoacoustic signal generated only by the energy transfer process described before and assuming that $\beta_{F_2^-}(\lambda)$ and $F_{F_2^-}(\lambda)$ can be approximated by $\beta_{F_2^-}(\bar{\lambda})$ and $F_{F_2^-}(\bar{\lambda})$, where $\bar{\lambda}$ corresponds to the F_3^- center emission band maximum.

Table 2
Luminescence quantum efficiency (LQE) for LiF:F₃⁻ crystals at 1.55 eV disregarding the energy transfer due to the overlapping of the F₃⁻ centers emission and the F₂⁻ centers absorption bands

Sample	F(1.55 eV)	LQE (η)
#1	0.34 ± 0.1	0.7 ± 0.2
#2	0.2 ± 0.1	0.9 ± 0.2
#3	0.28 ± 0.1	0.8 ± 0.2
#4	0.38 ± 0.1	0.7 ± 0.2

Table 3
Luminescence quantum efficiency (LQE) for LiF:F₃⁻ crystals at 1.55 eV considering the energy transfer due to the overlapping of the F₃⁻ centers emission and the F₂⁻ centers absorption bands

Sample	F(1.55 eV)	LQE (η)
#1	0	1.1 ± 0.2
#2	0	1.1 ± 0.2
#3	0.2 ± 0.1	0.9 ± 0.2
#4	0.28 ± 0.1	0.8 ± 0.2

Then

$$I_{PA,F_3^-}(\lambda) = A \{1 - \exp[-\beta_{F_3^-}(\lambda)l]\} \times \{F_{F_3^-}(\lambda) + [1 - F_{F_3^-}(\lambda)] \times \{1 - \exp[-\beta_{F_2^-}(\bar{\lambda})l]\} F_{F_2^-}(\bar{\lambda})\} \quad (13)$$

and the ratio of Eqs. (9) and (13) allows the determination of $F_{F_3^-}(\lambda)$ and $\eta_{F_3^-}(\lambda)$, shown in Table 3.

These values are the real ones for the sample studied. The obtained values for F_3^- centers in samples 1 and 2 (see Table 3) do not correspond to the expected ones, since the minimum acceptable value for F_3^- , under the employed model, and considering the LQE equal to one (see Eq. (3)), is $F_{F_3^-}(1.55 \text{ eV}) = 0.1$. The errors on these results are due to the difficulties in obtaining the experimental values from the spectra, mainly from the photoacoustic spectra where the spectral decomposition in gaussians was rendered difficult due to the background noise. Considering the $F_{F_3^-}$ values for samples 3 and 4 and by comparing them to the corresponding ones in Table 2 it was estimated that 8% of the energy absorbed by the F_3^- centers is transferred to the F_2^- centers in sample 3 (F_2^-/F_3^- absorption ratio at the peak equal to 1.5) and 10% in sample 4 (F_2^-/F_3^- absorption ratio at the peak equal to 2). Extrapolation of this result for a sample having equal F_3^- and F_2^- centers concentration led to a 5% energy transfer value.

5. Conclusions

The results obtained for the LQE of LiF:F₂⁻ crystals, shown in Table 1, agree with the values from 0.3 to 0.5 reported by Basiev [1] but disagree from the 0.22 value at room temperature reported by Gellermann [10]. These values are the only ones reported

in the literature and the discrepancy among these values evince the difficulties in obtaining the LQE.

In the present work it was not observed any influence of the irradiation process (γ or electrons), centers concentration or the relative concentration of F_2^- to F_3^- centers on the LQE value. The obtained LQE value, not close to the unity, is unexpected since other deexcitations mechanisms, besides the luminescent radiative decay, are unknown. A possible nonradiative mechanism occurring is the quenching due to other centers [11]. This supposition was strengthened by the observation of F_2^- centers formation in the LiF crystal studied, with concentration around 10^{17} /mol, only when high F centers (10^{20} /mol) and F_2 centers (10^{18} /mol) concentrations were present. Another possible extrinsic parameter was the presence of impurities in the crystal, like OH^- and Mg^{++} , with concentrations of the same order as of the F_2^- centers, 10 ppm. Since the F_2^- center in LiF is very stable even not having local electric charge compensation, it should have some mechanism of charge compensation like an association with a cationic impurity. This association would be responsible for the observed stability and could affect the center deexcitation mechanism.

The energy transfer from the F_3^- centers to the F_2^- centers in LiF crystals allowed the LQE determination using a different and indirect methodology, without the need to know the excitation spectrum of the F_3^- centers, although with a considerable statistical error in the measurements evinced by the obtained results. The high LQE obtained, 0.9 ± 0.2 , was expected, since other deexcitation mechanisms besides the luminescence are unknown. Considering the mechanism of energy transfer, extrapolation of our results for a sample having equal F_3^- and F_2^- centers

concentration led to a 5% energy transfer value. Although the LQE for the F_3^- centers in LiF is high, its application as a laser medium or a Q-switching element in a laser cavity is rendered difficult due to its low thermal stability [2]. This is the first reported LQE value for F_3^- centers in LiF.

Acknowledgements

We acknowledge Dr. Sergey Mirov, from the General Physics Institute, for two of the LiF: F_2^- samples studied. We also thank CNPq/RHAE for the scholarship for M. Duarte.

References

- [1] T.T. Basiev, S.B. Mirov and V.V. Osiko, *IEEE J. Quantum Electron* 24 (1988) 1052.
- [2] V.A. Archangelskaya and A.E. Poletimov, *Opt. Spectrosc. (USSR)* 57 (1984) 227.
- [3] A.E. Hughes, *Solid State Commun.* 4 (1966) 337.
- [4] A. Rosencwaig and E.A. Hildum, *Phys. Rev. B* 23 (1981) 3301.
- [5] Y. Ohba, M. Mizuta and H. Kukimoto, *J. Lum.* 28 (1983) 111.
- [6] J. Hamilton, I. Duncan and T. Morrow, *J. Lum.* 33 (1985) 1.
- [7] F.A. McDonald and G.C. Wetsel Jr., *J. Appl. Phys.* 49 (1978) 2313.
- [8] A. Rosencwaig and A. Gersho, *J. Appl. Phys.* 47 (1976) 64.
- [9] W. de Rossi, F.E. Costa, N.D. Vieira Jr., N.U. Wetter, S.P. Morato, T.T. Basiev, V.A. Konyushkin and S.B. Mirov, *Appl. Optics* 31 (1992) 2719.
- [10] W. Gellermann, A. Muller and D. Wandt, *J. Appl. Phys.* 61 (1987) 1297.
- [11] G. Baldacchini, in: *Advances in Nonradiative Processes in Solids*, ed. B. di Bartolo (Plenum Press, New York, 1991) p. 219.